A mode-locked external-cavity quantum-dot laser with a variable repetition rate*

Wu Jian(吴 剑), Jin Peng(金 鹏)†, Li Xin-Kun(李新坤), Wei Heng(魏 恒), Wu Yan-Hua(吴艳华), Wang Fei-Fei(王飞飞), Chen Hong-Mei(陈红梅), Wu Ju(吴 巨), and Wang Zhan-Guo(王占国)

Key Laboratory of Semiconductor Materials Science and Beijing Key Laboratory of Low-dimensional Semiconductor Materials and Devices, Institute of Semiconductors, Chinese Academy of Sciences, Beijing 100083, *China*

(Received 23 March 2013; revised manuscript received 25 April 2013)

A mode-locked external-cavity laser emitting at 1.17-μm wavelength using an InAs/GaAs quantum-dot gain medium and a discrete semiconductor saturable absorber mirror is demonstrated. By changing the external-cavity length, repetition rates of 854, 912, and 969 MHz are achieved respectively. The narrowest −3-dB radio-frequency linewidth obtained is 38 kHz, indicating that the laser is under stable mode-locking operation.

Keywords: quantum dot, mode-locked laser, external cavity

PACS: 42.60.Fc, 78.67.Hc, 81.07.Ta, 81.16.Dn **DOI:** 10.1088/1674-1056/22/10/104206

1. Introduction

Mode-locked semiconductor lasers[1–3] generating ultrashort pulse trains are suitable for a wide range of applications, such as optical sampling,[4] clock recovery and frequency conversion,[5] optical time-division multiplexing,[6] and optical coherence tomography.[7] Self-assembled quantum-dots (QDs) with broad gain bandwidth and ultrafast gain and absorption recovery time are ideal materials for fabricating mode-locked lasers.[8–13] The self-assembled QDs grown by the Stranski–Krastanow mode possess a broad distribution of dot sizes. Such a size inhomogeneity of the self-assembled QDs can broaden the width of the gain spectrum.[14–18] Although the shortest pulse duration obtained in mode-locked QD lasers is 312 fs[9] at present, QD material has the potential for generating sub-100-fs pulses[6] due to the broadened gain bandwidth if all the gain bandwidth is coherently employed and the dispersion effect is minimized. Such a broadened width of the gain spectrum is also useful for realizing broadband tuning of the output wavelengths.[18–29] Meanwhile, QD material has the advantage of a lower saturation fluence than quantum-well material,[30] which enables it to serve as the optimum saturable absorption material in mode-locked lasers. Moreover, QD material exhibits a ultrafast recovery time under both absorption and gain conditions.[31] This ultrafast carrier dynamics allows QD material to produce high repetition-rate pulse trains. 238-GHz repetition rate has been demonstrated in a mode-locked QD laser by harmonic mode-locking method.[32] The data show that the QD mode-locked laser is also well suited to high-speed optoelectronic applications.

The external-cavity (EC) configuration offers some advantages compared with monolithic devices. The flexibility of EC configuration overcomes monolithic mode-locked lasers' invariability of repetition rate. Monolithic mode-locked laser's inability to generate relatively low repetition-rate pulses can be settled easily by using an EC mode-locked laser, since the EC configuration largely extends the cavity length of the laser system. Furthermore, appropriate optical elements can be introduced to realize wavelength tuning and dispersion compensation for pulse narrowing. Choi *et al*,[33] reported on the first mode-locked EC QD laser in 2005. This two-section device operated at repetition rates of 2.4 GHz–6.0 GHz and produced highly chirped 15-ps pulses. Using an external dual-grating dispersion compensator, the pulse duration was compressed down to 1.2 ps. Instead of using a two-section device, McRobbie *et al*.[34] in 2007, realized an all QD EC mode-locked laser based on a QD gain device and a QD semiconductor saturable absorber mirror (SESAM) as the discrete mode-locking element. This mode-locked EC QD laser generated pulse repetition rates ranging from 350 MHz to 1.5 GHz, with an average output power up to 27 mW (860 MHz). More recently, a mode-locked EC QD laser has been demonstrated with a pulse repetition rate from a record-low value of 191 MHz to 1 GHz.[33]

In the present paper, we fabricate a gain device using self-assembled InAs/GaAs QDs as its active region. Then an SESAM-coupled mode-locked EC QD laser is constructed

*Project supported by the National Natural Science Foundation of China (Grant Nos. 61274072, 60976057, and 60876086).

†Corresponding author. E-mail: pengjin@semi.ac.cn

© 2013 Chinese Physical Society and IOP Publishing Ltd

with the QD gain device. Stable mode-locking is achieved under different injection current conditions, with an average power of up to 20 mW. By changing the total cavity length, repetition rates of 854, 912, and 969 MHz are achieved, respectively.

2. Experiment

The mode-locked EC QD laser, shown in Fig. 1, comprises a simple linear EC configuration, combined with a QD gain device, a collimating lens, a focusing lens, and an SESAM. The epitaxial structure of the QD gain device is similar to that described in our previous paper.[17] It was grown on an n-GaAs (001) substrate by a Riber 32P solid-source molecular beam epitaxy machine. The active region contained ten layers of self-assembled InAs QDs, each of which was covered by a 2-nm thick InGaAs cap layer and separated from the adjacent QD layers by a GaAs spacer layer. Below and above the waveguide were 1.5-μm n-type and 1.5-μm p-type $Al_{0.5}Ga_{0.5}As$ cladding layers, respectively. Finally, a 300-nm thick p^+-GaAs layer was capped as an Ohmic contact layer. Then the QD epitaxial chip was processed to fabricate the gain device using standard photolithography and a wet etching process. The gain device had a ridge waveguide structure with a waveguide width of 5 μm and a device length of 1.5 mm. Both facets were coated: a single $\lambda/4$ SiO_2 anti-reflection (AR) layer designed to minimize the reflectivity at 1.16 μm was deposited on one facet; SiO_2/Ta_2O_5 double layers were deposited on the other facet with a designed reflectivity of 20% at the same wavelength. Finally, the gain device was mounted p-side down on a copper heat sink.

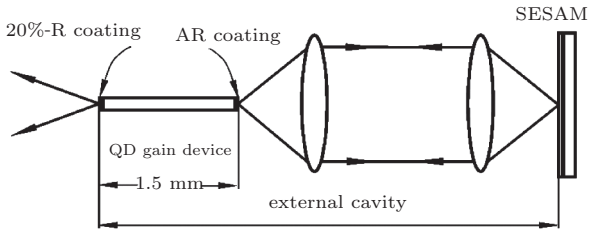


Fig. 1. Configuration of the mode-locked EC QD laser.

Light emission from the AR-coated facet was coupled into the EC using an 8-mm focal-length collimating lens, and then focused onto the SESAM using another 8-mm focal-length focusing lens. The saturation fluence of the SESAM (Batop SAM-1150-6) was around 60 μJ/cm^2 and the reflectivity exceeded 94% for wavelengths ranging from 1.11 μm to 1.19 μm. By varying the distance between the collimating and focusing lens, the total cavity length could be changed accordingly, resulting in changing the repetition rate without spoiling the stable mode-locking operation. Mode-locked pulses were detected by a high-speed InGaAs photodetector whose output signal was connected to a radio-frequency (RF) spectrum analyzer with a bandwidth of 3 GHz. Measurements of emission spectrum, light power, and RF spectrum were all performed under continuous-wave (CW) current injection at room temperature. In this paper, the power value measured by a pyroelectric probe is the average power of the mode-locked pulses, not the peak one.

3. Results and discussion

In order to investigate the mode-locking performance at different fundamental repetition rates, the optical lengths of the EC (which were calculated by including the refractive indices of the gain device and the two lenses) are set to be 175, 165, and 155 mm, respectively. Light power–current (*P*–*I*) properties of the free-running gain device and mode-locked EC lasers are shown in Fig. 2(a). Threshold currents of the mode-locked EC lasers are much smaller than that of the free-running gain device. This can be attributed to the high reflectivity of the SESAM, which greatly reduces the cavity loss. For all the three different cavity-length EC lasers, stable mode-locking was observed by RF spectrum analyzer, which will be discussed below, from 120-mA current and could be maintained until 140-mA current, resulting in output power up to 20 mW. Figure 2(b) shows the normalized electroluminescent (EL) spectra of the mode-locked EC lasers under 130-mA current. For comparison, normalized EL spectra of the free-running gain device under 10, 20, 50, 100, and 180-mA current are presented. From Fig. 2(c), a blue shift of emission spectra can be observed with the increase of current from 10 mA to 100 mA. This phenomenon can be attributed to the inhomogeneity of the QDs' size distribution and the effect of carries transferring between different dots. At a low injection level, carries in small dots can escape out of them and transfer to large ones which have lower energy levels. Therefore, under this current, carries mainly occupy the ground-states (GSs) of the large dots and radiate in the long-wavelength region. When the injection level increases, the GSs of the large dots with a relatively small amount may soon approach to saturation and then carries will gradually fill the small dots' GSs, leading to the blue shift of the emission wavelength. As the current further increases, lasing occurs at 1.15 μm where the sufficient dots with the corresponding size can provide enough gain to overcome the cavity loss. By contrast, the EC configuration has a relatively small cavity loss. The relaxed gain requirement enables the EC laser to achieve lasing at a relatively long wavelength (around 1.17 μm) as shown in Fig. 2(b).

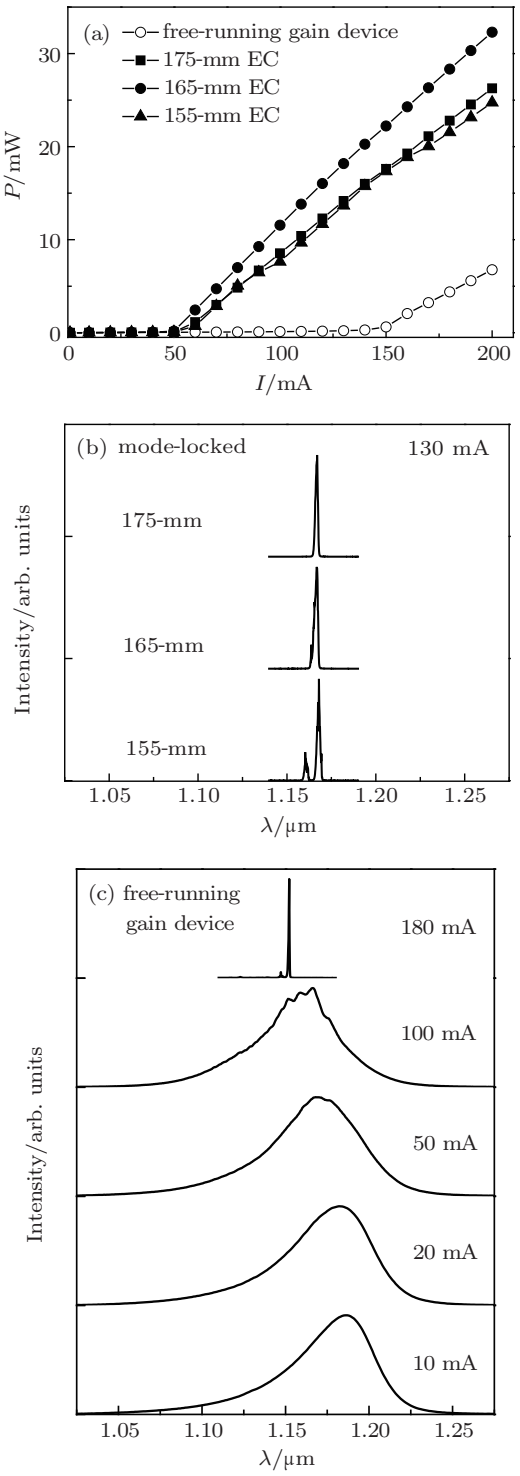


Fig. 2. (a) Light power–current (P–I) curves of the free-running gain device and mode-locked EC lasers measured from the 20%-reflectivity facet; (b) normalized EL spectra of the mode-locked EC lasers under 130-mA current; (c) normalized EL spectra of the free-running gain device under 10, 20, 50, 100, and 180-mA current.

Figure 3 shows the RF spectra of the mode-locked EC QD lasers. The repetition rate f, which equals the reciprocal of the pulse's cavity round-trip time, strictly depends on the optical length of the total cavity L, i.e.,

$$f = \frac{c}{2L}, \tag{1}$$

where c denotes the speed of light in vacuum. Therefore, a shorter cavity length leads to a higher repetition rate. Repetition rates of 854, 912, and 969 MHz were realized respectively for the 175-, 165-, and 155-mm EC optical length. Under 120-mA current, the −3-dB RF linewidth of 38 kHz was obtained in the 165-mm EC configuration and its RF spectrum demonstrated that the signal-to-noise ratio was larger than 30 dB, showing the low noise and robust stability for mode-locking operation as shown in Fig. 4.

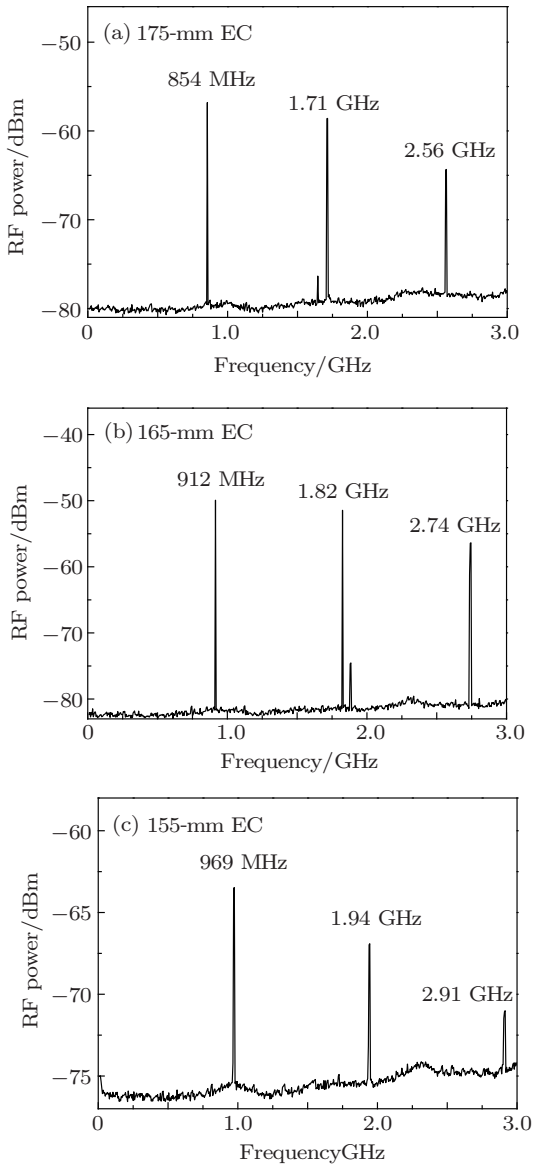


Fig. 3. (a) RF spectral trace for 854-MHz mode-locking under 120-mA current, measured with a resolution bandwidth of 100 kHz; (b) RF spectral trace for 912-MHz mode-locking under 120-mA current, measured with a resolution bandwidth of 51 kHz; (c) RF spectral trace for 969-MHz mode-locking under 120-mA current, measured with a resolution bandwidth of 300 kHz.

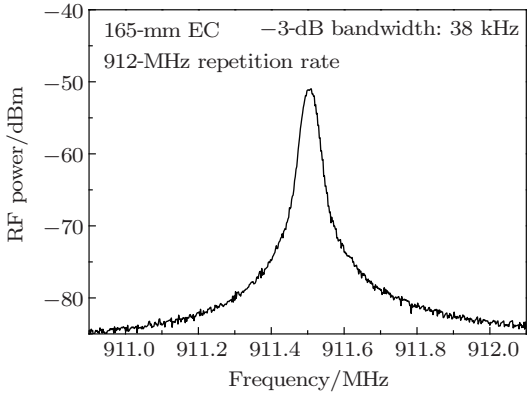


Fig. 4. 1.2-MHz-span RF spectral trace around 912-MHz fundamental mode-locking frequency under 120-mA current, measured with a resolution bandwidth of 30 kHz.

The output pulse energy E_p can be obtained from the following formula:

$$E_p = \frac{P_{out}}{f}, \tag{2}$$

where P_{out} and f denote the average output power and the repetition rate, respectively. Under the sable mode-locking condition (120 mA–140 mA), the output pulse energy range of the three different cavity-length lasers can be calculated out as shown in Table 1. If we neglect the loss of the SESAM, the intra-cavity pulse energy E_{intra} incident on the SESAM should meet the following two equations during a round trip in the cavity:

$$E_p = E_{intra} g_{gain}(1-R), \tag{3}$$

$$E_{intra} = E_{intra} g_{gain}^2 R, \tag{4}$$

where g_{gain} is the single-path gain of the gain device and R is the reflectivity of the output facet, which is 20% for the gain device. So we have

$$E_{intra} = E_p \cdot \frac{\sqrt{R}}{1-R}. \tag{5}$$

We can deduce that the intra-cavity pulse energy E_{intra} is around 56% of the output pulse energy E_p, as listed in Table 1. Based on the structure of the gain device, we estimate that the effective mode area on the facet is about 3 μm^2. The incident light area on the SESAM should be comparable to this value if we neglect the diffraction of the two lenses. Dividing the previously obtained E_{intra} by this 3 μm^2, we can calculate the pulse fluence F_{intra} incident on the SESAM. In order to compare this pulse fluence with the saturation fluence F_{sat} (= 60 μJ·cm^{-2}) of the SESAM, the values of their ratio F_{intra}/F_{sat} which is usually defined as the saturation parameter S are also listed in Table 1.

Typically, the SESAM operates with a saturation parameter S from 3 to 5,[7] since the mode-locked laser can produce the shortest pulse duration under such a condition.[34] For weaker or stronger absorber saturation condition, the pulse duration will become longer. The experimentally estimated ranges of S for the three different cavity-length mode-locked EC lasers are close to that of the ideal condition.

Table 1. Pulse parameters for different cavity-length mode-locked EC lasers.

EC length/mm	E_p/pJ	E_{intra}/pJ	$F_{intra}/10^2$ μJ·cm^{-2}	S
175	14–19	7.8–11	2.6–3.7	4.3–6.2
165	18–22	10–12	3.3–4.0	5.5–6.7
155	12–16	6.7–9.0	2.2–3.0	3.7–5.0

4. Conclusion

A straight-waveguide gain device emitting at 1.15 μm using self-assembled InAs/GaAs QDs as its active region is fabricated. By employing this gain device and a discrete SESAM, a mode-locked EC QD laser emitting at 1.17 μm is achieved to operate separately with repetition rates of 854, 912, and 969 MHz. Stable mode-locking with an average power up to 20 mW is measured at a repetition rate of 912 MHz, corresponding to 22-pJ output pulse energy. The experimentally estimated range of the saturation parameter S is 3.7–6.7, which is close to that of the ideal condition.

References

[1] Ho P T, Glasser L A, Ippen E P and Haus H A 1978 *Appl. Phys. Lett.* **33** 241
[2] Huang X D, Stintz A, Li H, Lester L F, Cheng J L and Malloy K J 2001 *Appl. Phys. Lett.* **78** 2825
[3] Yoshita M, Kuramoto M, Ikeda M and Yokoyama H 2009 *Appl. Phys. Lett.* **94** 061104
[4] Yamada N, Ohta H and Nogiwa S 2002 *Electron. Lett.* **38** 1044
[5] Delfyett P, Hartman D and Ahmad S 1991 *J. Lightwave Technol.* **9** 1646
[6] Rafailov E U, Cataluna M A and Sibbett W 2007 *Nat. Photon.* **1** 395
[7] Keller U 2003 *Nature* **424** 831
[8] Rafailov E U, Cataluna M A, Sibbett W, Zadiranov Y M, Zhukov A E, Ustinov V M, Livshits D A, Kovsh A R and Ledentsov N N 2005 *Appl. Phys. Lett.* **87** 81107
[9] Lu Z G, Liu J R, Raymond S, Poole P J, Barrios P J and Poitras D 2008 *Opt. Express* **16** 10853
[10] Thompson M G, Rae A R, Xia M, Penty R V and White I H 2009 *IEEE J. Quantum Electron.* **15** 661
[11] Cataluna M A, Rafailov E U, McRobbie A D, Sibbett W, Livshits D A and Kovsh A R 2006 *IEEE Photon. Technol. Lett.* **18** 1500
[12] Liu J R, Lu Z G, Raymond S, Poole P J, Barrios P J and Poitras D 2008 *Opt. Lett.* **33** 1702
[13] Nikitichev D, Ding Y, Ruiz M, Calligaro M, Michel N, Krakowski M, Krestnikov I, Livshits D, Cataluna M and Rafailov E 2011 *Appl. Phys. B* **103** 609
[14] Liu N, Jin P and Wang Z G 2012 *Chin. Phys. B* **21** 117305
[15] Li X K, Liang D C, Jin P, An Q, Wei H, Wu J and Wang Z G 2012 *Chin. Phys. B* **21** 028102
[16] Liang D C, An Q, Jin P, Li X K, Wei H, Wu J and Wang Z G 2011 *Chin. Phys. B* **20** 108503
[17] Wu J, Lü X Q, Jin P, Meng X Q and Wang Z G 2011 *Chin. Phys. B* **20** 064202
[18] Lü X Q, Jin P and Wang Z G 2010 *Chin. Phys. B* **19** 018104
[19] Lü X Q, Jin P and Wang Z G 2010 *IEEE Photon. Technol. Lett.* **22** 1799
[20] Lü X Q, Jin P, Wang W Y and Wang Z G 2010 *Opt. Express* **18** 8916

[21] Varangis P M, Li H, Liu G T, Newell T C, Stintz A, Fuchs B, Malloy K J and Lester L F 2000 *Electron. Lett.* **36** 1544

[22] Li H, Liu G T, Varangis P M, Newell T C, Stintz A, Fuchs B, Malloy K J and Lester L F 2000 *IEEE Photon. Technol. Lett.* **12** 759

[23] Eliseev P, Li H, Stintz A, Liu G T, Newell T C, Malloy K J and Lester L F 2000 *IEEE J. Quantum Electron.* **36** 479

[24] Biebersdorf A, Lingk C, De Giorgi M, Feldmann J, Sacher J, Arzberger M, Ulbrich C, Böhm G, Amann M C and Abstreiter G 2003 *J. Phys. D: Appl. Phys.* **36** 1928

[25] Allen C Nì, Poole P J, Barrios P, Marshall P, Pakulski G, Raymond S and Fafard S 2005 *Physica E* **26** 372

[26] Ortner G, Allen C Nì, Dion C, Barrios P, Poitras D, Dalacu D, Pakulski G, Lapointe J, Poole P J, Render W and Raymond S 2006 *Appl. Phys. Lett.* **88** 121119

[27] Tierno A and Ackemann T 2007 *Appl. Phys. B* **89** 585

[28] Nevsky A Yu, Bressel U, Ernsting I, Eisele Ch, Okhapkin M, Schiller S, Gubenko A, Livshits D, Mikhrin S, Krestnikov I and Kovsh A 2008 *Appl. Phys. B* **92** 501

[29] Fedorova K A, Cataluna M A, Krestnikov I, Livshits D and Rafailov E U 2010 *Opt. Express* **18** 19438

[30] Maas D J H C, Bellancourt A R, Hoffmann M, Rudin B, Barbarin Y, Golling M, Südmeyer T and Keller U 2008 *Opt. Express* **16** 18646

[31] Borri P, Schneider S, Langbein W and Bimberg D 2006 *J. Opt. A: Pure Appl. Opt.* **8** S33

[32] Rae A R, Thompson M G, Penty R V, White H I, Kovsh A R, Mikhrin S S, Livshits D A and Krestnikov I L 2006 *Proceedings of the* 19*th IEEE LEOS Annual Meeting*, July 17–19, 2006, Quebec City, Canada, p. 874

[33] Ding Y, Cataluna M A, Nikitichev D, Krestnikov Igor, Livshits D and Rafailov E 2011 *Appl. Phys. Express* **4** 062703

[34] Paschotta R and Keller U 2001 *Appl. Phys. B* **73** 653